IMPEDANCE STUDY WITH SINGLE BUNCH BEAM AT TAIWAN PHOTON SOURCE

C. C. Kuo, P. J. Chou, K. T. Hsu, K. H. Hu, C. Y. Liao, C. C. Liang,
Z. K. Liu, H. J. Tsai, F. H. Tseng
National Synchrotron Radiation Research Center, Hsinchu 30076, Taiwan

Abstract

The impedance at Taiwan Photon Source was investigated. The effects of bunch current such as a tune change, a synchronous phase shift and a bunch lengthening under operation conditions at various stages were measured; the machine impedances were deduced. This report presents the results with insertion devices in various configurations.

INTRODUCTION

The Phase-I beam commissioning of Taiwan Photon Source (TPS) was achieved with a stored beam up to 100 mA (limited by two normal-conducting cavities) in 2015 March. The maximum single-bunch current attained up to 12 mA. The bunch length and tune shift were measured as functions of the bunch current also in 2015 March. A preliminary analysis of the ring impedance with dummy chambers of full gap 20 mm vertically in the straight sections for insertion devices (ID) has been reported [1].

Several months were required to install ten Phase-I IDs and to replace the RF systems with superconducting modules in mid 2015. The Phase-II beam commissioning of TPS began in September [2, 3]. Abnormal vacuum events in the chamber of Cell-2 prevented an increased beam accumulation (< 300 mA.) In November, a dipole chamber of Cell-2 was removed and replaced with a new one; a burned screw and a melted plastic cap were found on the bottom of this chamber. After the replacement of the chamber, we attained 520 mA in December, above the design value 500 mA. User trial runs began in 2016 March.

Of ten ID, three are elliptically polarized undulators (EPU) and seven are in-vacuum undulators (IU). These three EPU have chambers of racetrack shape; the inner vertical dimension is full gap 8 mm. The seven IU can be closed to full gap 7 mm. ID chambers have special tapers to keep the transitions as smooth as practicable. We conducted measurements of bunch length, synchronous phase, beam size (energy spread) and tune shift vs bunch current up to 10 mA (single bunch) with varied configurations of the ID gaps.

The computer simulations of the TPS broad-band impedance were reported [4, 5]. The measurement results of the real machine are discussed in this article.

LONGITUDINAL IMPEDANCE

The longitudinal broad-band coupling impedance of the ring elements are divisible into real and imaginary components [6]. The real part is the sum of the resistive components and is characterized as the loss factor that represents the synchronous phase shift to compensate for energy loss and the skewness of the longitudinal bunch profile due to wake fields; the imaginary part perturbs the particle motion inside the bunch and results in bunch lengthening or shortening, a synchrotron tune shift and an energy spread.

Synchronous Phase Shift

To extract the resistive part of the impedance, a lock-in amplifier (Zurich Instruments, UHFLI) was employed in the synchronous phase-detection system, shown in Fig. 1.

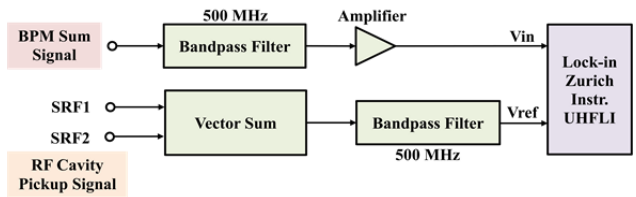

Figure 1: Synchronous phase detection of TPS.

The loss factor of the coupling impedance is expressible as $k_{\|} = V_{RF}\cos(\phi_s)\Delta\phi_s(f_0/I_b)$, in which V_{RF} denotes the RF voltage, ϕ_s the synchronous phase, f_0 the revolution frequency and I_b the bunch current. For a Gaussian bunch, $k_{\|} = R/(2\sqrt{\pi}\sigma_z^a)$, in which R is the resistive component in a R and L (inductive as most light sources) series-circuit model, σ_z is the bunch length and a is a machine-dependent scaling parameter.

Figure 2 depicts the measured synchronous phase shift vs bunch current at varied RF voltage after the IDs were installed. The measured loss factor as a function of bunch current is shown in Fig. 3; scaling factor a ranges from 1.17 to 1.21. The resistive component R is shown in Table 1. The loss factor is larger for a gap open as shown in Table 1 and Fig. 2. Measured temperature rise in the taper area with 40 mm gap was larger than 7 mm. There might be some trapped modes.

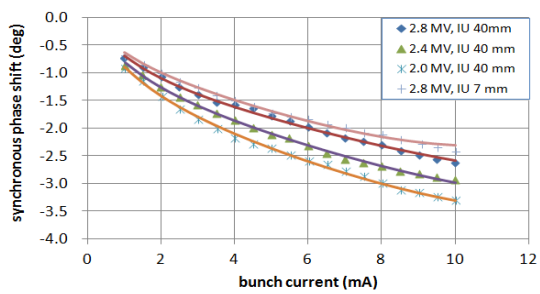

Figure 2: Measured synchronous phase shift of TPS with varied RF voltage and in-vacuum undulator gap.

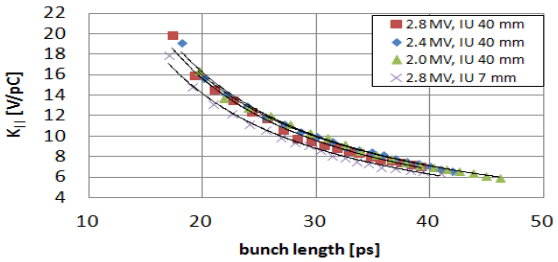

Figure 3: Measured longitudinal loss factor $k_{\|}$ vs bunch length σ_z of TPS; $k_{\|} \sim \sigma_z^{-a}$, a =1.17~1.21.

Bunch Lengthening

In a diagnostic beam line from a bending port, there exist an X-ray pinhole camera and an interferometer to measure the beam size, and a streak camera branch in the visible light regime to detect the bunch length [7]. A dual-sweep streak camera (C10910 Hamamatsu Photonics) is equipped to measure the longitudinal motion of the beam and the bunch length with picosecond resolution.

The impedance causes a distortion of the potential well (PWD); the equilibrium distribution generated by the wake fields of the bunch charges are described approximately with the Haissinski equation [8],

$$\lambda(z) = A\exp\left(-\frac{z^2}{2\sigma_{z0}^2} + \frac{1}{V'_{rf}\sigma_{z0}^2}\int_0^z V_{ind}(z')dz'\right)$$

in which $V_{ind}(z) = -\int_0^\infty W_{\|}(z')\lambda(z-z')dz'$, $W_{\|}(z')$ is the longitudinal wake fields, A is a normalization factor, V'_{rf} is the slope of the rf and σ_{z0} is the zero-current bunch length. The induced voltage is approximated as a combination of λ and λ', and is modeled in a series combination of fixed R and fixed L [9]

$$V_{ind} = -eNc(R\lambda + cL\lambda')$$

The Haissinski equation thus becomes solvable numerically with an iterative method.

Figure 4 shows the rms bunch length vs bunch current at varied RF gap voltage and ID gap setting.

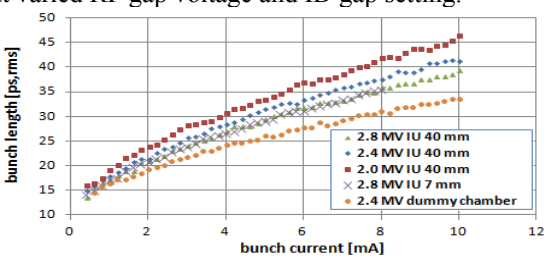

Figure 4: Measured bunch length of TPS with varied ID chambers and gaps of all seven in-vacuum undulators.

The measured energy spread of the beam deduced from measurements of the beam size is depicted in Fig. 5, indicating that the microwave instability threshold is about 3.0 mA for 2.0 MV RF. The instability occurring about 8.2 mA might be due to a strong horizontal head-tail instability in the case with chromaticity (x, y) = (1.2, 3.0), and was damped on increasing the chromaticity to (1.9, 4.0). The vertical beam size did not change up to 10 mA.

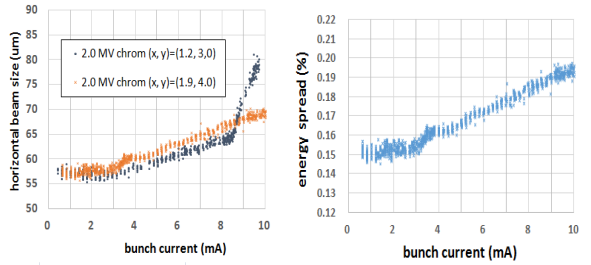

Figure 5: Measured horizontal beam size (left) and energy spread (right) vs bunch current with RF 2.0 MV and chromaticity (x, y) = (1.2, 3.0) and (1.9, 4.0). The threshold of the microwave instability is about 3 mA. About 8.2 mA, there is an instability due to a strong head-tail mode that is damped on increasing the horizontal chromaticity to about 1.9.

Cubic Fit of the Potential-Well Distortion

Zotter's bunch lengthening for the PWD [10,11] is

$$\left(\frac{\sigma_z}{\sigma_{z0}}\right)^3 - \frac{\sigma_z}{\sigma_{z0}} = \frac{1}{\sqrt{2\pi}}\frac{\alpha_c e I_b}{E_0 \nu_{s0}^2}\left(\frac{c}{\omega_0 \sigma_{z0}}\right)^3 \mathrm{Im}\left(\frac{Z_{\|}}{n}\right)_{eff}$$

and turbulent bunch lengthening is

$$\sigma_z{}^3 = \frac{1}{\sqrt{2\pi}}\frac{\alpha_c e I_b}{E_0 \nu_{s0}^2}\left(\frac{c}{\omega_0}\right)^3 \mathrm{Im}\left(\frac{Z_{\|}}{n}\right)_{eff}$$

in which E_0 denotes the beam energy, ν_{s0} the synchrotron frequency, ω_0 the revolution frequency, α_c the momentum compaction factor, I_b the average bunch current, and $\mathrm{Im}(Z_{\|}/n)_{eff}$ the imaginary effective longitudinal impedance.

Fitting below the microwave threshold, we obtained the imaginary part of the impedance; the results are listed in Tables 1~2 and Fig. 7. If we fit the turbulence regime, the impedance increases by a factor about 1.6. The effects of the ID chamber and the obstacle are clearly shown.

RL Circuit Model Fit

The resistances R obtained from measurement of the synchronous phase shifts, as listed in Table 1, were employed in the model fits of the RL series circuit in a bunch profile to produce inductive impedance L. Figure 6 shows the measured longitudinal profiles for varied bunch currents below the microwave instability threshold (~2.4 mA) at RF voltage 2.8 MV with IU gaps open. The effective machine impedance is expressed as $\mathrm{Im}|Z_{\|}/n|_{\mathrm{eff}} = \omega_0 L$. The results of the RL model fit in the bunch profile, as well as $\mathrm{Im}|Z/n|_{\mathrm{eff}}$, are given in Table 1. Using the RL circuit model and taking resistive R from the synchronous phase measurements and inductive L from the bunch profile fit, the bunch length is obtained, shown in Fig. 7. The inductive impedance fitting in the turbulence region also results in a factor about 1.5 larger than PWD regime.

ISBN 978-3-95450-147-2

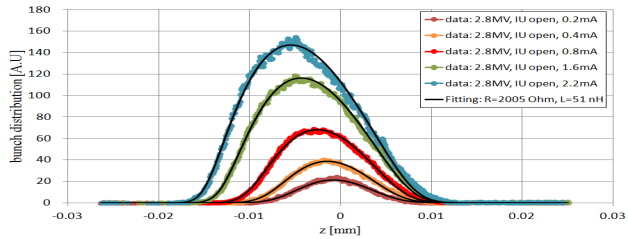

Figure 6: Measured and model fitted bunch profiles at varied bunch current below the threshold of microwave instability for the case with RF voltage 2.8 MV and IU gaps open.

The results from Zotter's cubic equation satisfactorily agree with the RL model. Figure 7 shows the measured and model fitted bunch lengths with Zotter's and the RL model in the case with RF 2.8 MV and IU open.

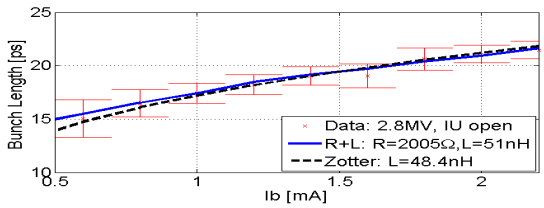

Figure 7: Measured and model fitted bunch length as a function of bunch current at the TPS storage ring below the threshold of microwave instability.

Table 1: Measured loss factor at zero current from the synchronous phase shift and deduced broad-band impedance from a model fit for varied RF voltage and IU gap.

IU gap (mm)		40	40	40	7
RF (MV)		2.8	2.4	2.0	2.8
σ_{z0} (ps)		10.77	11.74	13.07	10.81
$k_{\|\|}$ (V/pC)		33.11	30.68	26.56	29.13
R (Ω)		2005	1893	1794	1530
R+L	L (nH)	51	49	50	44
	$\|Z_{\|\|}/n\|_{\text{eff}}$ (Ω)	0.185	0.178	0.182	0.167
Zotter	L (nH)	48.4	46.9	50.8	44.8
	$\|Z_{\|\|}/n\|_{\text{eff}}$ (Ω)	0.176	0.170	0.185	0.163

Table 2: Broad-band Impedance Fitted from the Zotter Equation

Date	$\|Z_{\|\|}/n\|_{\text{eff}}$ (Ω)	Note
2015.03.26	0.093	dummy chambers, 20 mm
2015.11.19	0.197	2 EPU 8 mm, 7 IU open, cell-2 screw before removal
2015.12.16	0.177	2 EPU 8 mm, 7 IU open, cell-2 after screw removal
2015.12.16	0.163	2 EPU 8 mm, 7 IU, gap 7 mm

TRANSVERSE IMPEDANCE

The short-range transverse wake fields generated by the transverse broad-band impedance can interact resonantly with the bunched beam and result in a transverse mode coupling, or a strong head-tail instability; a positive chromaticity is consequently needed to damp the unstable beam. To attain a stable beam more than 10 mA, the chromaticity of the TPS storage ring was required to be about 2.0 and 4.0 in the horizontal and vertical planes, respectively. We measured the betatron tune shift as a function of bunch current up to 10 mA for various machine conditions, as shown in Fig. 8 for the vertical plane. Although the vertical frequency shift is across several synchrotron frequencies at large beam current and chromaticity is not zero, we applied the formula from [6,12]

$$\frac{\Delta\nu_{x,y}}{\Delta I}=\frac{c^2}{4\sqrt{\pi}(E/e)\nu_{x,y}\omega_0^2\sigma_s}\mathrm{Im}(Z_\perp^{x,y})_{eff}$$

to obtain the transverse effective impedance, and obtained $(Z_\perp^y)_{eff}$ =0.175 MΩ/m at zero current for a dummy chamber and 0.292 MΩ/m with ID installed and IU with gap 7 mm. Horizontal tune shift is very small and accuracy is not enough.

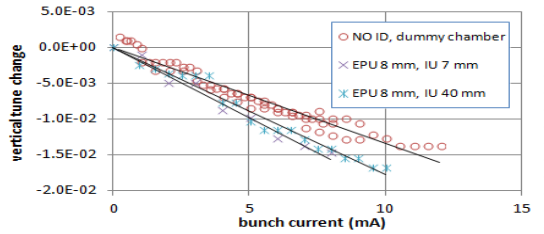

Figure 8: Measured vertical tune shift vs bunch current.

DISCUSSION

The loss factor and effective longitudinal impedance of the TPS storage ring were deduced from the synchronous phase shift, bunch length and bunch profile measurements with a single-bunch beam; the results are compatible with the preceding computer simulations. An effective longitudinal impedance that increased in the presence of an obstacle in the chamber and the addition of ID was observed. The threshold of microwave instability was about 3 mA for RF 2.0 MV, which agrees satisfactorily with the result of computer simulation. The impedance fit in the turbulence region resulted in an increase by factor 1.6 over the PWD. One possible reason is that PWD is sensitive to Z/n near the frequency of the bunch spectrum; turbulence is sensitive to higher frequencies and turbulence fit results in total impedance in two regions [10]. The effective transverse impedance also increased on adding ID.

ACKNOWLEDGEMENT

We thank A.W. Chao of SLAC for advice on this work. We appreciate also the assistance of the Instrumentation and Control Group and operation staff.

REFERENCES

[1] C. C. Kuo, et al., "Commissioning of the Taiwan Photon Source", Proc. IPAC 2015, TUXC3, p.1314.
[2] M. S. Chiu, et al., "Commissioning of Phase-I Insertion Devices in TPS", IPAC 2016, THPMB050, these proceedings.

[3] Ch. Wang, et al., "System Integration and Beam Commissioning of the 500-MHz RF systems for Taiwan Photon Source", IPAC 2016, WEPMB052, these proceedings.
[4] A. Rusanov, "Impedance Study for the TPS Storage Ring", Proc. IPAC 2010, TUPD057, p.2060.
[5] A. Rusanov and P. J. Chou, "Collective Effects Simulations for the TPS Storage Ring", Proc. IPAC 2010, TUPD058, p.2063.
[6] A. Chao, "Physics of Collective Beam instabilities in High Energy Accelerators", Wiley, New York, 1993.
[7] C. Y. Liao et al., "Synchrotron Radiation Measurement at Taiwan Photon Source", Proc. IBIC2015, 2015, TUPB067.
[8] J. Haissinski, "Exact Longitudinal Equilibrium Distribution of Stored Electrons in the presence of a self-field", Nuovo Cimento, Vol. 18B, No. 1 (1973).
[9] K. L. F. Bane et al., "Impedance Analysis of Bunch Length Measurements at the ATF Damping Ring", SLAC-PUB-8846, 2001.
[10] B. Zotter, in "Handbook of Accelerator Physics and Engineering", edited by A. Chao and M. Tigner, World Scientific, Singapore, 2013, p146, 2nd edition.
[11] J. Corbett, et al., "Bunch Length and Impedance Measurements at SPEAR3", Proc. EPAC08. 2008, TUPP028, p.1595.
[12] A.-S. Muller, et al., "Studies of Current-dependent Effects at ANKA", Proc. EPAC04. 2004, p.2011.

ISBN 978-3-95450-147-2